Journal of Alloys and Compounds 508 (2010) 79–84

Contents lists available at ScienceDirect

Journal of Alloys and Compounds

journal homepage: www.elsevier.com/locate/jallcom

The phase relationships in the Al–Zr–Ho ternary system at 773 K

Mingjun Pang[a], Yongzhong Zhan[a,*], Wenchao Yang[a], Chunliu Li[a], Yong Du[b]

[a] Laboratory of Nonferrous Metal Materials and New Processing Technology, Ministry of Education, Guangxi University, Nanning, Guangxi 530004, PR China
[b] State Key Laboratory of Powder Metallurgy, Central South University, Changsha, Hunan 410083, PR China

ARTICLE INFO

Article history:
Received 10 August 2010
Accepted 14 August 2010
Available online 24 August 2010

Keywords:
Metals and alloys
Phase diagrams
X-ray diffraction

ABSTRACT

The phase relationships in the Al–Zr–Ho ternary system at 773 K have been investigated in the whole compositional range. The existences of 13 binary compounds, i.e. Al_3Zr, Al_2Zr, Al_3Zr_2, AlZr, Al_3Zr_4, Al_2Zr_3, $AlZr_2$, $AlZr_3$, $AlHo_2$, Al_2Ho_3, AlHo, Al_2Ho and Al_3Ho have been confirmed. $Al_{17}Ho_2$ was not found at 773 K in this work. In addition, the ternary compound $Al_{15}Ho_4Zr$ is confirmed. It has $AuCu_3$ structure and its lattice parameter is $a = 0.4201$ nm. The results show that the isothermal section consists of 17 single-phase regions, 32 two-phase regions and 16 three-phase regions. The solubility of Zr in Al_2Ho, AlHo and Ho is about 71 at.%, 6 at.% and 12 at.% Zr, respectively. No remarkable solid solubility could be found in the other compounds of the Al–Zr–Ho ternary system at 773 K.

1. Introduction

Al–RE (RE = rare earth) alloys have attracted great interests in recent years due to their specific properties and possibility of commercial application [1–4]. These more properties come from intermetallic compounds in the system. For example, metallic compounds of Al_3Sm or Al_3Dy can significantly lower the resistivity of the alloy [2] and Al_3Sc plays an important role in improving the strength of Al–Sc alloy [3]. It is well known that most of rare earth elements have good magnetism. The results of Zaremba et al. [5] showed that the effective magnetic moment for Ce^{3+}, Pr^{3+} and Nd^{3+} has small difference between fitted and theoretical values. It means that the effective magnetic moment of RE^{3+} has a very good locality. For the Al–RE alloys, rare earth elements always exist in RE^{3+} or RE^{2+} states. Therefore, it can be deduced that Al–RE intermetallic compounds hold some magnetic performance in a certain degree.

Raquet et al. [6] have studied the magnetic and transport properties in high magnetic field of holmium/zirconium multilayers. They found that there is a sharp magnetic transition because of the closing of the conical or helical configurations as in bulk material. However, it disappears for the lower thicknesses of Ho layers and the transition field changes with the magnetic coupling through the zirconium layers. It demonstrates that the coupling of magnetic and nonmagnetic component can cause magnetic transition.

Though Zr is a nonmagnetic element, it plays an important role in magnetic materials. It is reported that the addition of Zr can not only improve the thermal stability [7] but also obtain high magnetic properties [8]. In order to develop new lightweight alloys for magnetic applications, it is necessary to study the Al–Zr–RE phase diagram. Recently, Al–Zr–RE (RE = Y, Pr and Ce) phase diagram [9–11] are reported. Ho is one of the most important rare earth magnetic elements, but very few reports can be found on the Al–Zr–Ho system.

In the Al–Zr binary system [12], there are eight binary compounds, i.e. Al_3Zr, Al_2Zr, Al_3Zr_2, AlZr, Al_3Zr_4, Al_2Zr_3, $AlZr_2$ and $AlZr_3$ at 773 K. According to Ref. [13], five compounds, i.e. $AlHo_2$, Al_2Ho_3, AlHo, Al_2Ho and Al_3Ho exist in the Al–Ho binary phase diagram. Pop et al. [14] first reported a new intermetallic compound $Al_{17}Ho_2$ in 1993 and then Huang et al. [15] also found it in Al–Ti–Ho system at 773 K. However, it is not found in the Al–B–Ho [16], Al–Cu–Ho [17] and Al–Ho–Mg [18] systems. It is reported that there is no binary compound found in Zr–Ho binary phase diagram [19]. The crystal structure data of the phases in the Al–Zr–Ho system at 773 K are given in Table 1.

At the early time, Tyvanchuk and Protsyk [22] determined the isothermal section of the Al-rich corner of the Al–Zr–Ho ternary system at 773 K. But in order to show completely the phase relationship of this system, we investigated the whole isothermal section at 773 K by means of X-ray powder diffraction (XRD) and differential thermals analysis (DTA) to provide information for materials design and calculation of phase diagrams.

2. Experimental procedure

All the alloy samples were produced by arc melting on a water-cooled copper cast with a non-consumable tungsten electrode under pure argon atmosphere. Titanium was used as O_2 getter during the melting process. Each sample was prepared with a total weight of 1.5 g by weighing with purity of Al 99.99 wt.%, Zr 99.95 wt.% and Ho 99.95 wt.%. Each arc-cast button was turned around after each melting and then melted three times for better homogeneity. For most alloys, the weight loss is less than 1% after melting.

* Corresponding author. Tel.: +86 771 3272311; fax: +86 771 3233530.
E-mail address: zyzmatres@yahoo.com.cn (Y. Zhan).

0925-8388/$ – see front matter © 2010 Elsevier B.V. All rights reserved.
doi:10.1016/j.jallcom.2010.08.058

Table 1
Crystal structure data for the phases at 773 K in the Al–Zr–Ho system [13,20,21].

Phase	Crystal structure	Space group	Pearson symbol	Prototype	Strukturbericht	Lattice parameters (nm)		
						a/α[a]	b/β[a]	c/γ[a]
(Al)	Cubic	$Fm\bar{3}m$	*cF*4	Cu	*A*1	0.40496		
(Ho)	Hexagonal	$P6_3/mmc$	*hP*2	Mg	*A*3	0.35778		0.56178/120°
(αZr)	Hexagonal	$P6_3/mmc$	*hP*2	Mg	*A*3	0.32316		0.51475/120°
Al_3Zr	Tetragonal	$I4/mmm$	*t*/16	Al_3Zr	$D0_{23}$	0.4005		1.7285
Al_2Zr	Hexagonal	$P6_3/mmc$	*hP*12	$MgZn_2$	C14	0.52824(5)		0.87482(5)/120°
Al_3Zr_2	Orthorhombic	*Fdd*2	*oF*40	Al_3Zr_2		0.9601(2)	1.3906(2)	0.5574(2)
AlZr	Orthorhombic	*Cmcm*	*oC*8	CrB	B_f	0.3353	1.0866	0.4266
Al_3Zr_4	Hexagonal	$P\bar{6}$	*hP*7	Al_3Zr_4		0.5433(2)		0.5390(2)/120°
Al_2Zr_3	Tetragonal	$P4_2/mnm$	*tP*20	Al_2Zr_3		0.7630(1)		0.6998(1)
$AlZr_2$	Hexagonal	$P6_3/mmc$	*hP*6	Ni_2In	$B8_2$	0.4894		0.5928/120°
$AlZr_3$	Cubic	$Pm\bar{3}m$	*cP*4	$AuCu_3$	$L1_2$	0.43917(1)		
$AlHo_2$	Orthorhombic	*Pnma*	*oP*12	Co_2Si	*C*23	0.6528	0.5053	0.9347
Al_2Ho_3	Tetragonal	$P4_2/mnm$	*tP*20	Al_2Zr_3		0.8182		0.7525
AlHo	Orthorhombic	*Pbcm*	*oP*16	AlEr		0.5801	1.1339	0.5621
Al_2Ho	Cubic	$Fd\bar{3}m$	*cF*24	Cu_2Mg	*C*15	0.7816(3)		
Al_3Ho	Hexagonal	$R\bar{3}m$	*hR*20	Al_3Ho		0.6052		3.5930/120°
$Al_{15}Ho_4Zr$	Cubic	$Pm\bar{3}m$	*cP*4	$AuCu_3$		0.421		

[a] The degrees of the missing α, β, γ angle are equal to 90°.

All the melted alloy buttons were sealed in evacuated quartz tubes for homogenization heat treatment. The heat treatment temperature was determined by differential thermal analysis (DTA) or based on previous work of the three binary phase diagrams. The alloys at the Al-rich corner were homogenized at 873 K for 20 days and the rest alloys were homogenized at 1073 K for 1 month, then cooled down to 773 K at a rate of 9 K/h and maintained for more than 1 week.

Finally, all these annealed alloys were quenched in liquid nitrogen. The equilibrated samples were ground into powder and then analyzed on a Rigaku D/Max-2500 V diffractometer with Cu Kα radiation and graphite monochromator. The scan ranges of the samples were from 20° to 60° (2θ) with a speed of 10°/min. The software Jade 5.0 and Powder Diffraction File (PDF release 2003) [23] were used for phase identification.

3. Results and discussion

3.1. Isothermal section

The isothermal section of the Al–Zr–Ho ternary system at 773 K has been determined mainly on the basis of XRD, as is shown in Fig. 1. This isothermal section consists of 16 three-phase regions, 32 two-phase regions and 17 single-phase regions. The Al-rich corner of this work agrees well with Ref. [22].

Constitutions of the three-phase regions and compositions of the typical alloys are listed in Table 2. The XRD results confirmed that 13 binary and 1 ternary compounds, namely Al_3Zr, Al_2Zr, Al_3Zr_2, AlZr, Al_3Zr_4, Al_2Zr_3, $AlZr_2$, $AlZr_3$, $AlHo_2$, Al_2Ho_3, AlHo, Al_2Ho, Al_3Ho and $Al_{15}Ho_4Zr$ exist in this system at 773 K.

The XRD patterns of some representative samples located in some three-phase regions are shown in Figs. 2–4. Fig. 2 illustrates the XRD pattern of the sample $Al_{0.57}Zr_{0.17}Ho_{0.26}$ located in the Al_3Zr + AlHo + Al_2Ho three-phase region. Based on the analysis of the XRD pattern (shown in Fig. 3), there is three phases (i.e. Al_2Ho_3, Al_2Zr_3 and Al_3Zr_4) in the sample with the atomic proportion of Al 41%, Zr 32% and Ho 27%. Fig. 4 indicates clearly the existence of three phases (Ho, Al_2Zr_3 and $AlHo_2$) in the equilibrated sample with the atomic proportion of Al 20%, Zr 15% and Ho 65%.

3.2. Phase analysis

3.2.1. Binary system

In the Al–Zr system, this work confirms eight binary compounds at 773 K, i.e. $AlZr_3$, $AlZr_2$, Al_2Zr_3, Al_3Zr_4, AlZr, Al_3Zr_2, Al_2Zr and Al_3Zr, which agrees well with the work in Ref. [12]. The present work also identifies that the Al_3Zr_5 and Al_4Zr_5 phases do not exist in this system. It can be seen from Fig. 5 that the XRD pattern of the samples (35 at.% Al. 60 at.% Zr and 5 at.% Ho) consists of three phases,

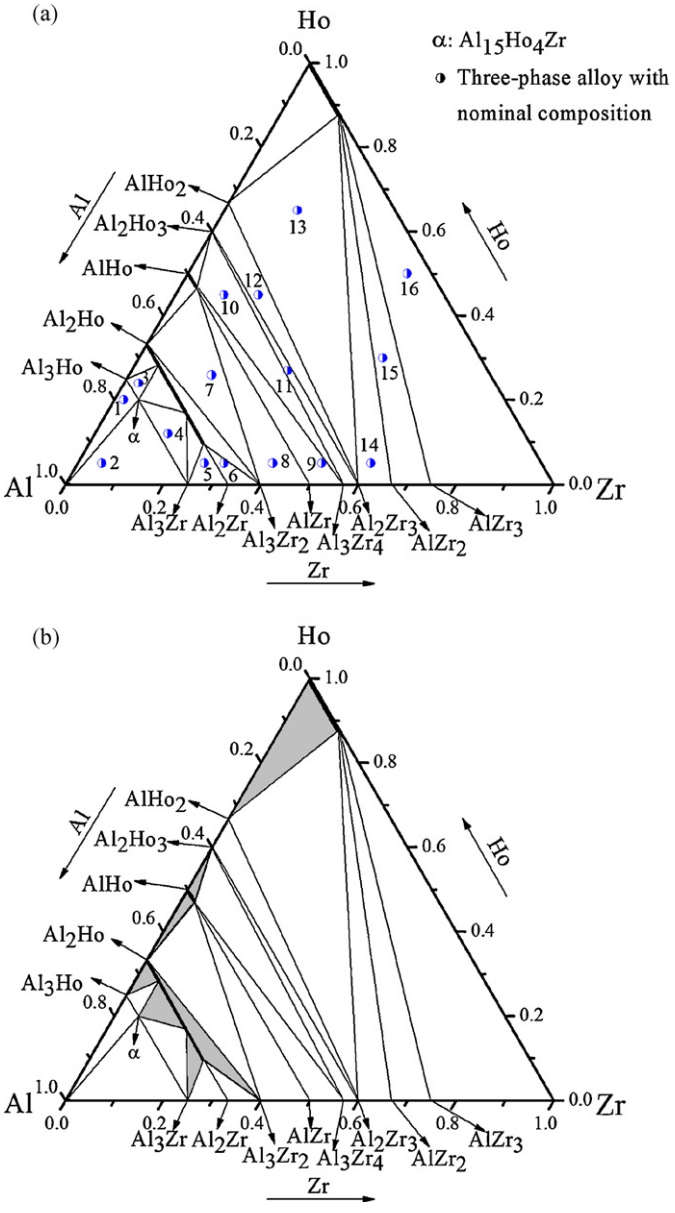

Fig. 1. Isothermal section of the Al–Zr–Ho ternary system at 773 K: (a) with the present typical experimental data; (b) without the experimental data.

Table 2
Summary of three-phase alloy composition, identified phases, phase compositions and lattice parameters for the Al–Zr–Ho alloys at 773 K.

No.	Chemical composition (at.%)			Phase analysis[a]	Lattice parameters (nm)		
	Al	Zr	Ho		a/α[b]	b/β[b]	c/γ[b]
1	78	2	20	Al Al_3Ho $Al_{15}Ho_4Zr$	0.4039 0.6026		 3.5780/120°
2	90	5	5	Al Al_3Zr $Al_{15}Ho_4Zr$	 0.4010		 1.7289
3	73	3	24	Al_3Ho $Al_{15}Ho_4Zr$ Al_2Ho	 0.4201		
4	73	15	12	Al_3Zr $Al_{15}Ho_4Zr$ Al_2Ho	 0.7820		
5	69	26	5	Al_3Zr Al_2Ho Al_2Zr	 0.5282		 0.8755/120°
6	65	30	5	Al_2Ho Al_2Zr Al_3Zr_2	 0.9612	 1.3952	 0.5589
7	57	17	26	Al_2Ho AlHo Al_3Zr_2	 0.5739	 1.1325	 0.5576
8	55	40	5	AlZr AlHo Al_3Zr_2	0.3407	1.0776	0.4284
9	45	50	5	AlZr AlHo Al_3Zr_4	 0.5411		 0.5401/120°
10	45	10	45	Al_2Ho_3 AlHo Al_3Zr_4	0.8174		0.7478
11	41	32	27	Al_2Ho_3 Al_3Zr_4 Al_2Zr_3	 0.7678		 0.7008
12	38	17	45	Al_2Zr_3 Al_2Ho_3 $AlHo_2$	 0.6501	 0.5044	 0.9336
13	20	15	65	Al_2Zr_3 $AlHo_2$ Ho	 0.3579		 0.5628/120°
14	35	60	5	Al_2Zr_3 $AlZr_2$ Ho	 0.4913		 0.5914/120°
15	20	50	30	Ho $AlZr_2$ $AlZr_3$	 0.4381		
16	5	45	50	Ho Zr $AlZr_3$	 0.3239		 0.5180/120°

[a] The identified phases for all alloys are measured with XRD.
[b] The degrees of the missing α, β, γ angle are equal to 90°.

i.e. Ho, $AlZr_2$ and Al_2Zr_3. The results of this work are in accordance with Refs. [9–11].

For the Al–Ho system, the existence of five binary compounds i.e. $AlHo_2$, Al_2Ho_3, AlHo, Al_2Ho and Al_3Ho are confirmed in this work. The XRD pattern of the alloy with atomic proportion of 89.47 at.% Al and 10.53 at.% Ho shows that $Al_{17}Ho_2$ does not exist at 773 K (Fig. 6).

The present work indicates that no binary compound exists in the Ho–Zr system, which agrees well with the results of Ref. [19]. The XRD pattern of the sample (5 at.% Al, 45 at.% Zr, 50 at.% Ho) indicates the existence of Ho, Zr and $AlZr_3$, as shown in Fig. 7.

3.2.2. Ternary compound of $Al_{15}Ho_4Zr$

The ternary compound $Al_{15}Ho_4Zr$ in the system and its crystal structural data have been reported [22]. It has $AuCu_3$ structure (space group $Pm\bar{3}m$) with lattice parameter $a = 0.421$ nm. It is also confirmed in the present isothermal section. In this work, the XRD pattern of the equilibrated sample which contains 75 at.% Al, 20 at.% Ho and 5 at.% Zr clearly indicates the existence of the $Al_{15}Ho_4Zr$ single-phase, as illustrated in Fig. 8. From Fig. 9, it can be observed that there are three phases in the equilibrated sample with 78 at.% Al, 2 at.% Zr and 20 at.% Ho at 773 K, i.e. $Al_{15}Ho_4Zr$, Al_3Ho and Al. In addition, it also clearly indicates that three phases exist in the

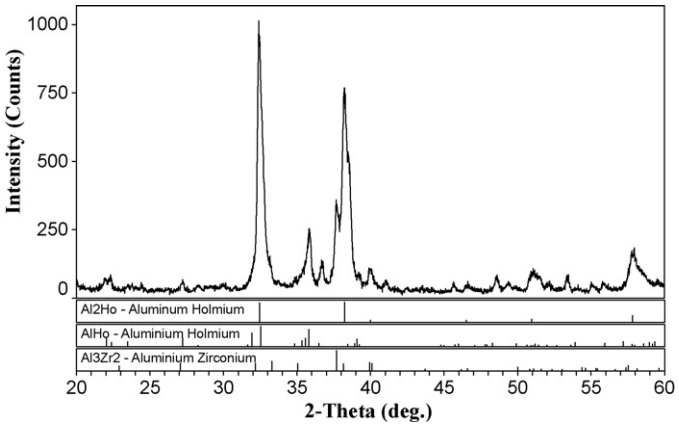

Fig. 2. The XRD pattern of the equilibrated sample prepared with the atomic proportion of Al 57%, Zr 17% and Ho 26%.

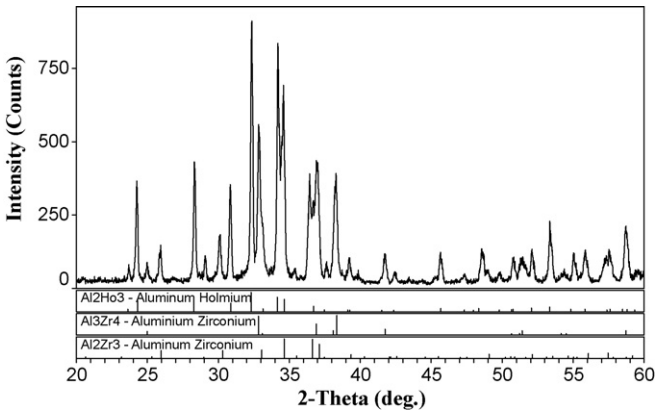

Fig. 3. The XRD pattern of the equilibrated sample prepared with the atomic proportion of Al 41%, Zr 32% and Ho 27%.

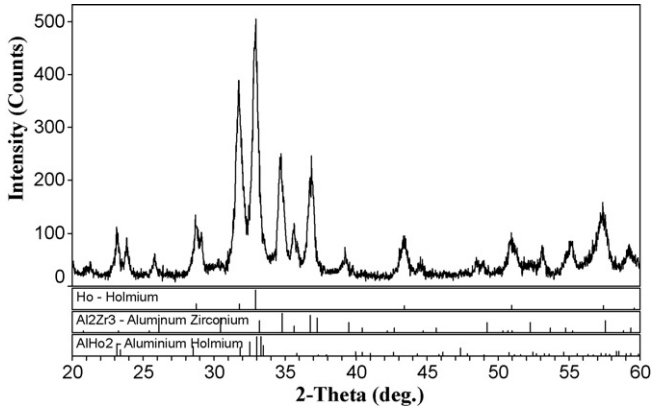

Fig. 4. The XRD pattern of the equilibrated sample prepared with the atomic proportion of Al 20%, Zr 15% and Ho 65%.

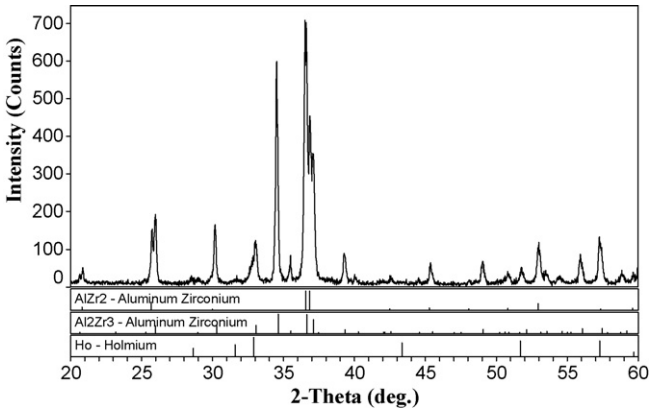

Fig. 5. The XRD pattern of the equilibrated sample prepared with atomic proportion of 35% Al. 60% Zr and 5% Ho.

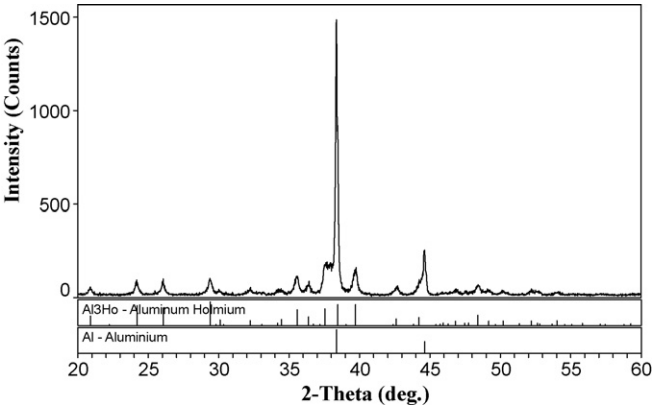

Fig. 6. The XRD pattern of the equilibrated sample prepared with atomic proportion of 10.53% Al and 89.47% Ho.

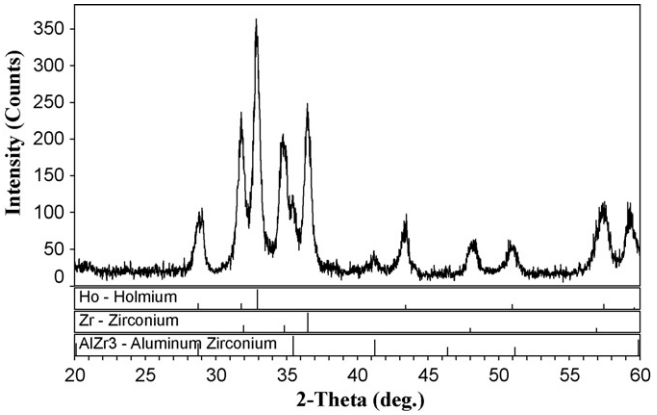

Fig. 7. The XRD pattern of the equilibrated sample prepared with atomic proportion of 5% Al, 45% Zr and 50% Ho.

sample with 90 at.% Al, 5 at.% Zr and 5 at.% Ho, i.e. $Al_{15}Ho_4Zr$, Al_3Zr and Al, as is shown in Fig. 10. Therefore, it can be concluded that the $Al_{15}Ho_4Zr$ phase is a stable phase. In addition, the analysis result using Jade 5.0 indicates that the lattice parameter of compound $Al_{15}Ho_4Zr$ is $a = 0.4201$ nm.

3.3. Solid solubility

The solid solubility ranges in this isothermal section are determined using the phase-disappearing method, lattice parameter method and comparing the shift of the XRD pattern of the samples near the compositions of the binary phases [24].

The solid solubility of Zr in Al_2Ho at 773 K is determined in this work. The XRD patterns of $Al_2(Ho_{1-3x}Zr_{3x})$ ($x = 0$, 0.05, 0.125, 0.175, 0.2, 0.225, 0.25 and 0.275) are shown in Fig. 11. There is only one phase observed in the samples of $Al_2(Ho_{1-3x}Zr_{3x})$ when x is lower than 0.25. However, another phase is found in the samples of $Al_2(Ho_{1-3x}Zr_{3x})$ when x is equal to 0.25 and 0.275. The lattice parameters are then calculated by the method of extrapolation. Fig. 12 shows that the lattice parameters of $Al_2(Ho_{1-3x}Zr_{3x})$ ($x = 0$, 0.05, 0.125, 0.175, 0.2 and 0.225) decreases almost lin-

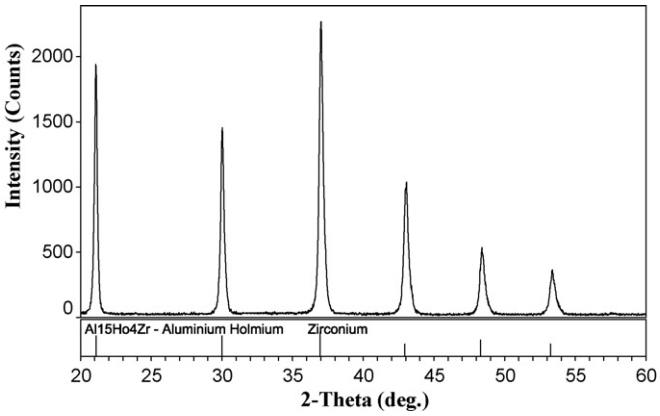

Fig. 8. The XRD pattern of the equilibrated sample (75 at.% Al, 20 at.% Ho and 5 at.% Zr) indicating the existence of the $Al_{15}Ho_4Zr$ single-phase.

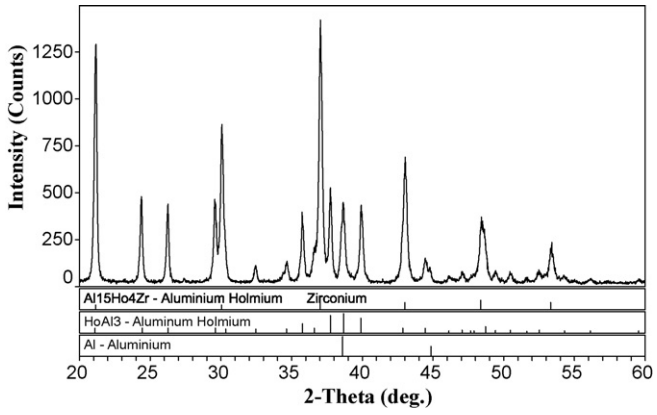

Fig. 9. The XRD pattern of the equilibrated sample (78 at.% Al, 2 at.% Zr and 20 at.% Ho) indicating the phase equilibrium of $Al_{15}Ho_4Zr$, Al_3Ho and Al.

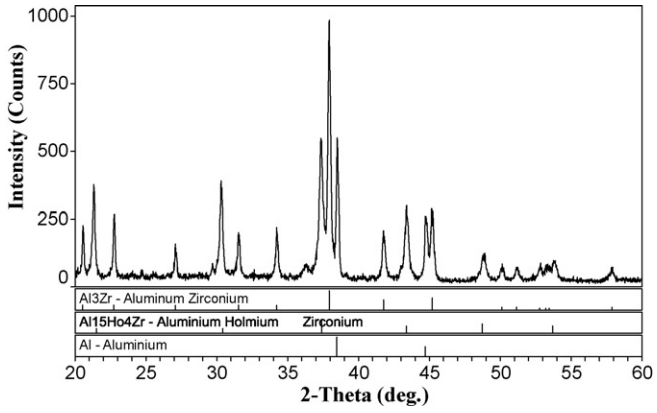

Fig. 10. The XRD pattern of the equilibrated sample (90 at.% Al, 5 at.% Zr and 5 at.% Ho) indicating the phase equilibrium of $Al_{15}Ho_4Zr$, Al_3Zr and Al.

early with increasing of Zr content, while the lattice parameter of $Al_2(Ho_{1-3x}Zr_{3x})$ ($x = 0.25$ and 0.275) remains constant. Therefore, the solid solution of Zr in Al_2Ho is estimated to range from 0 to 0.71.

In this work, samples of $Ho_{1-x}Zr_x$ ($x = 0.05$, 0.08, 0.09, 0.10, 0.11, 0.12, 0.13 and 0.14) are synthesized. The solid solubility of Zr in Ho at 773 K is determined by lattice parameter method. Fig. 13 shows the change of the lattice parameters of $Ho_{1-x}Zr_x$ ($x = 0.05$, 0.08, 0.09, and 0.10) with increasing of Zr content. When the content of Zr is in the range of 0–0.12, the lattice parameters of the compound decrease with increasing of Zr. However, when it is

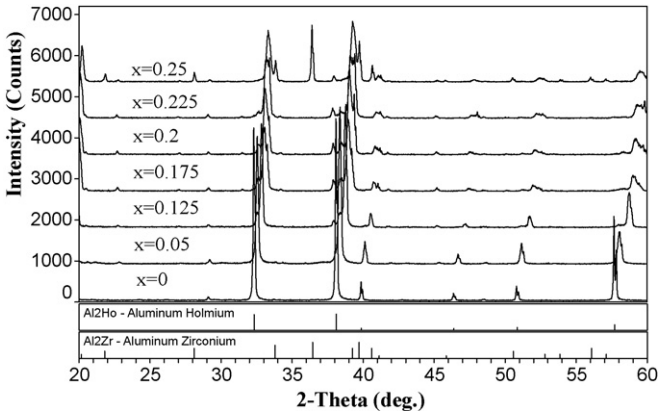

Fig. 11. The XRD patterns of the equilibrated alloys of $Al_2(Ho_{1-3x}Zr_{3x})$ ($x = 0$, 0.05, 0.125, 0.175, 0.2, 0.225, 0.25 and 0.275).

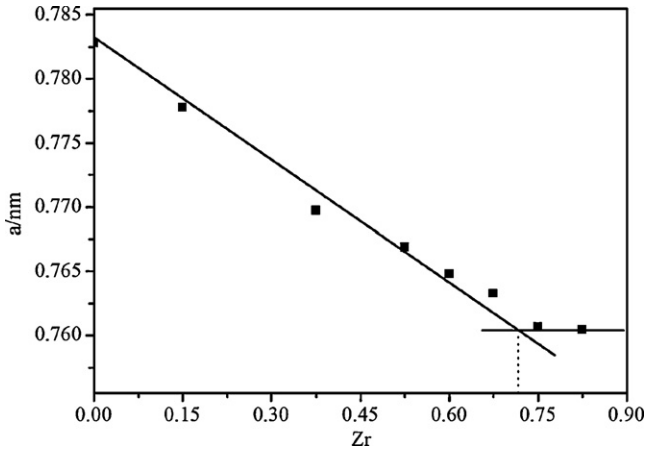

Fig. 12. The lattice parameters of $Al_2(Ho_{1-3x}Zr_{3x})$ ($x = 0$, 0.05, 0.125, 0.175, 0.2, 0.225, 0.25 and 0.275).

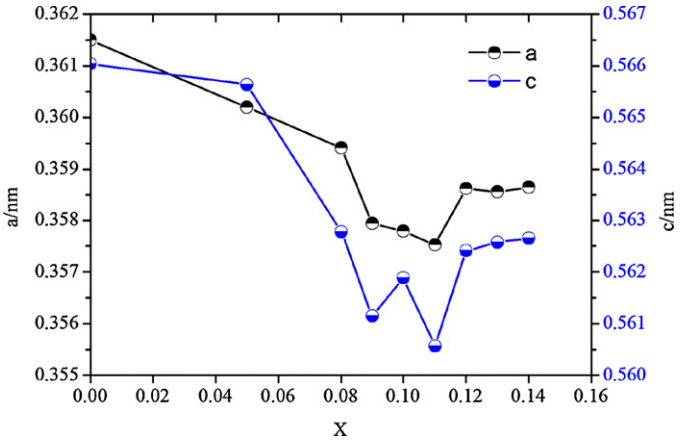

Fig. 13. Variations of the lattice parameters of $Ho_{1-x}Zr_x$ ($x = 0.05$, 0.08, 0.09, 0.10, 0.11, 0.12, 0.13 and 0.14) with the Zr content.

higher than 0.12, the lattice parameters of compounds tend to remain unchanged. It can be concluded that the solubility of Zr in Ho at 773 K is 0.12, which is close to the data reported in Ref. [19].

In addition, the results indicated that the solubility of Zr in AlHo was about 6 at.%. No remarkable solid solubility was found in mostly binary compounds at 773 K.

4. Conclusions

The isothermal section of the Al–Zr–Ho ternary system at 773 K is determined, which consists of 17 single-phase regions, 32 two-phase regions and 16 three-phase regions. The solubility of Zr in Al_2Ho, AlHo and Ho were about 71 at.%, 6 at.% and 12 at.% Zr, respectively. No remarkable solid solubility was found in mostly binary compounds at 773 K. In addition, the ternary compounds $Al_{15}Ho_4Zr$ is confirmed in this work and its lattice parameter is $a = 0.4201$ nm.

Acknowledgements

This research work is supported by National Natural Science Foundation of China (Grant No. 50831007).

References

[1] Z. Wang, Y. Li, J. Lee, Electrochem. Commun. 11 (2009) 1179–1182.
[2] S. Takayama, N. Tsutsui, Thin Solid Films 289 (1996) 289–294.
[3] Y. Ye, P. Li, L. Novikov, V. Avilkina, L. He, Acta Mater. 58 (2010) 2520–2526.
[4] M. Domínguez-Crespo, S. Rodil, A. Torres-Huerta, E. Ramírez-Meneses, G. Suárez-Velázquez, Surf. Coat. Technol. 204 (2009) 571–579.
[5] V.I. Zaremba, D. Kaczorowski, G.P. Nychyporuk, U.Ch. Rodewald, R. Pöttgen, Solid State Sci. 6 (2004) 1301–1306.
[6] B. Raquet, A. Sdaq, J. Broto, H. Rakoto, J. Ousset, S. Askenazy, A. Baudry, P. Boyer, M. Luche, A. Khmou, Physica B 211 (1995) 335–337.
[7] H. Ma, J. Zhang, G. Li, W. Zhang, W. Wang, J. Alloys Compd. (2010), doi:10.1016/j.jallcom.2010.04.075.
[8] J. Han, S. Liu, C. Wang, H. Chen, H. Du, Y. Yang, J. Magn. Magn. Mater. 321 (2009) 1331–1334.
[9] J. She, Y. Zhan, Z. Hu, C. Li, J. Hu, Y. Du, H. Xu, J. Alloys Compd. 497 (2010) 118–120.
[10] J. She, Y. Zhan, C. Li, Y. Du, H. Xu, Y He, J. Alloys Compd. (2010), doi:10.1016/j.jallcom.2010.05.004.
[11] Z. Hu, Y. Zhan, J. She, Y. Du, H. Xu, J. Alloys Compd. 491 (2010) 200–202.
[12] H. Okamoto, J. Phase Equilib. 23 (2002) 455–456.
[13] K.A. Gschneidner, Bull. Alloy Phase Diagrams 9 (1988) 684–685.
[14] I. Pop, M. Andrecut, I. Burda, Mater. Lett. 17 (1993) 79–83.
[15] J. Huang, J. Liang, H. Zhou, Y. Zhuang, J. Yan, J. Alloys Compd. 307 (2000) 199–201.
[16] V. Raghavan, J. Phase Equilib. Diffuse 28 (2007) 446–447.
[17] V. Raghavan, J. Phase Equilib. Diffuse 27 (2006) 151–152.
[18] V. Raghavan, J. Phase Equilib. Diffuse 28 (2007) 469–470.
[19] H. Okamoto, in: T.B. Massalski (Ed.), Binary Alloy Phase Diagrams, vol.3, II Ed., 1990, pp. 2232–2233.
[20] P. Villars, Pearson's Handbook of Crystallographic Data, ASM International, Materials Park, OH, 1997.
[21] J. Murray, J. Phase Equilib. 13 (1992) 277–290.
[22] A. Tyvanchuk, A. Protsyk, Dopov. Akad. Nauk Ukr. RSR, Ser. B 11 (1982) 60–62.
[23] Materials Data JADE Release 5.0, XRD Pattern Processing, Materials Data Inc., Livermore, CA, 2003.
[24] Y. Zhan, Y. Du, Y. Zhuang, Determination of Phase Diagrams Using Equilibrated Alloys, in: J.-C. Zhao (Ed.), Methods for Phase Diagram Determination, First ed., Elsevier Science Press, Amsterdam, The Netherlands, 2007, pp. 108–150.